Efficiency and Fairness Trade-Offs in SC-FDMA Schedulers

Kemal Davaslioglu, *Student Member, IEEE*, and Ender Ayanoglu, *Fellow, IEEE*

***Abstract*—In this paper, we address the uplink resource scheduling problem in single carrier frequency-domain multiple access systems. In particular, we focus on the efficiency and fairness trade-offs in scheduling and resource allocation for wireless cellular networks. We present an efficient implementation method that translates these scheduling problems into set partitioning problems that are well-studied in the literature. Then, we discuss a family of utility functions that enable us to investigate the performance of different frequency domain schedulers such as the sum-rate maximization, proportional fair, and max-min fair schedulers. We use the price of fairness as a metric to analytically quantify these trade-offs. Based on the intuition that fairness of resource allocation in cellular radio networks corresponds to the *prioritization* of cell-edge user rates, we demonstrate that the proportional fair scheduler significantly improves fairness among users, and increases the rates offered to the cell-edge and median users when compared to the sum-rate maximization scheduler. This comes at the cost of reducing the cell-center user rates and the aggregate user rate. We present the steps on how to take into account the practical implementation constraints, in particular, those related with the discrete Fourier transform implementation, in the problem formulation. Simulation results that illustrate these trade-offs are also presented. We conclude that this type of analysis can provide guidelines for the network operators to control the efficiency and fairness trade-off as the data traffic grows.**

***Index Terms*—Efficiency, fairness, integer programming, resource allocation, SC-FDMA, scheduling.**

I. Introduction

THE global mobile data traffic grew 70 percent in 2012 [1], and this trend is expected to continue in the next decade. These data rate demands are not only challenging to achieve, but also raise concerns on power consumption of next-generation wireless systems. In this paper, we address the concerns on efficiency, fairness, and power consumption for different schedulers. We discuss these in a Long-Term Evolution (LTE) system. LTE systems employ single carrier frequency domain multiple access (SC-FDMA) transmissions in the uplink transmissions to achieve high power-efficiency, improved coverage, and reduced power consumption at user equipments (UEs) [2]. This transmission scheme also provides a smaller peak-to-average power ratio (PAPR) compared to the orthogonal frequency division multiplexing access (OFDMA) that is used in the downlink, and thereby achieves significant cost and battery life savings for UEs.

In terms of resource management, there are four main algorithms in LTE. These are admission control, packet scheduling, power control, and interference control [2]. In this paper, we focus on the packet scheduling and power control algorithms. Let us note that LTE systems are designed to offer large flexibility in packet scheduling in time, frequency, and spatial domains. Through control channel signals, base stations schedule each transmission, so that the users are allocated orthogonal resources without any overlap. In order to keep the required signaling overhead manageable, especially for the uplink transmissions, the subcarriers are scheduled in groups in the frequency domain. Each subcarrier that occupies a bandwidth of 15 kHz is grouped in 12 subcarriers. These 12 subcarriers are called as a resource block (RB). Resource scheduling is then carried out with an allocation granularity of 180 kHz in the frequency domain [2, p. 78].

Frequency domain packet scheduling (FDPS) is a method used in LTE systems to allocate radio resources in the frequency domain such that the capacity of the system and the user experience are improved under some quality of service (QoS) and fairness constraints. When resource allocation for multiple users is considered, each user experiences different channel conditions and has different QoS requirements. FDPS allows assigning the resources such that the system performance can be optimized for different QoS requirements and efficiency versus fairness trade-offs. Typically, RBs are allocated to the users with the highest channel gains. Contrary to the best channel assignment strategy in OFDMA systems, only consecutive resources are assigned to users in SC-FDMA systems.

The works in [3], [4] investigate resource allocation problems in air traffic, health care, organ donor, and call center scheduling applications. In all these areas, utilities are shared among multiple users, and naturally, trade-offs between efficiency and fairness arise. The price of fairness is a metric introduced in [3], [4] to quantify the losses incurred to achieve fairness in the system. This metric can be used by the central decision maker to characterize and balance these trade-offs. Same observations can be made in scheduling and resource allocation in cellular radio networks. Especially, these trade-offs characterize the cell-edge user performance. In cases where the cell-center users are favored to increase the aggregate cell throughput, this may lead to cell-edge user rate starvation cases. In this paper, we use the price of fairness to characterize these trade-offs in an analytical framework.

Manuscript received July 1, 2013; revised October 31, 2013 and January 17, 2014; accepted March 11, 2014. The associate editor coordinating the review of this paper and approving it for publication was A. Vosoughi.

The authors are with the Center for Pervasive Communications and Computing, Department of Electrical Engineering and Computer Science, University of California, Irvine, CA 92697-2625, USA (e-mail: kdavasli@uci.edu, ayanoglu@uci.edu, ender.ayanoglu@gmail.com).

This work was partially supported by the National Science Foundation under Grant No. 1307551. Any opinions, findings, and conclusions or recommendations expressed in this material are those of the authors and do not necessarily reflect the view of the National Science Foundation.

Digital Object Identifier 10.1109/TWC.2014.042914.131176

Scheduling granularity per RB and contiguous resource assignment constraints provide significant benefits to reduce the control signal overhead and the search space of the SC-FDMA resource allocation problem. However, there are implementation constraints to be considered. In particular, we focus on the discrete Fourier transform (DFT) implementation constraints. The radices of DFT operations are typically chosen as prime factors [5]. In the early phases of the LTE standardization process, it was proposed to limit the DFT sizes to radices of 2, 3, and 5 [6].

A. Related Works

Related works in literature in channel dependent scheduling in SC-FDMA systems include [7]–[13]. It is shown in [7] that the FDPS problem in SC-FDMA systems with the contiguity constraint is NP-hard. The authors of [7] considered maximizing the proportional fair (PF) metric of users and presented four suboptimal algorithms with RB granularity. The same problem is also addressed in [8] on a per subcarrier basis where the authors presented two algorithms with different complexities. The first algorithm achieved the optimal solution with relatively high computational complexity, and the second yielded a suboptimal solution. The works in [9] and [10] proposed suboptimal greedy heuristic algorithms to maximize utility functions based on channel capacity and PF metrics, respectively. However, they did not consider the contiguity constraint. Another related work in [11] proposed three suboptimal algorithms based on the PF metric with RB granularity in varying levels of complexity. The efficiency and fairness of these schedulers are further studied in [12], [13]. In particular, the authors in [13] compared the performance of the heuristic algorithms presented in [7] and [11] to solve the sum-rate maximization (SRM) and PF scheduling problems. Although the work in [13] also identified the efficiency and fairness trade-offs in these schedulers, it did not quantify the efficiency losses or provide bounds for these trade-offs. We need to note that, unlike the heuristic solutions in [7] and [11]–[13], the work in our paper satisfies the optimality conditions, albeit with some increased complexity. Furthermore, the work in [13] considers a single-cell simulation setup whereas in our paper, we consider a more realistic multi-cell multiuser scenario that is proposed in the standards [14], [15].

The FDPS problem is also addressed in LTE downlink systems. The work in [16] presents linear programming (LP) solutions for various schedulers. The authors of [16] assume that the signal-to-noise-ratio (SNR) to the channel quality indicator (CQI) mapping for a fixed block error ratio (BLER) is linear. The study in [16] shows that the throughput can be estimated based on the uplink CQI feedback reports, and these estimates can be employed in the scheduling problem formulation. The constraint matrices of the LP problems in [16] are similar to those of [8] except for the contiguity constraint. Also, in [17] and [18], the authors present a cross-layer optimization framework for the utility-based scheduling problem in OFDM networks. The analysis in [17] considers an infinite number of subcarriers, whereas a finite number of subcarriers and more realistic conditions are investigated in [18]. The two-part paper [17], [18] studies the necessary and sufficient conditions for the dynamic subcarrier assignment (DSA), adaptive power allocation (APA), and their joint allocation schemes. The results in [17] identify that DSA offers a significant improvement over the fixed subcarrier assignment (FSA) scheme, while APA provides a limited improvement over FSA. The joint DSA and APA allocation has a marginal gain over the DSA scheme. However, in [18], with a finite number of subcarriers, the improvements of APA are more significant compared to the DSA scheme. This time, their joint allocation offers a substantial gain over both schemes. Since APA within RBs is not standardized in LTE systems, in this paper, we will only consider equal power allocation for the subcarriers in RBs. Similar to [18], we will also propose a DSA method in order to improve the sum utility of the users. In [19], the authors investigate the effects of finite and full buffer traffic models using the utility maximization framework in OFDMA networks. The study in [19] uses the same family of utility functions as in our paper. The results in [19] show that as the parameter characterizing the family of utility functions, α, decreases, the cell-edge user rates increase, and the authors propose to use a specific value of $\alpha = 0.6$ as the best trade-off point. As we will show in the sequel, as α increases, the fairness of user rates improves, and the fairness in wireless networks determines the cell-edge user rates [20]. The study in [19] also presents the gains of an α-fair scheduler over PF scheduler at different network loads. In our paper, along with a numerical study, we provide the upper bounds for these gains such that the network operator (as the decision maker) can make an informed decision on the efficiency and fairness trade-off before its implementation.

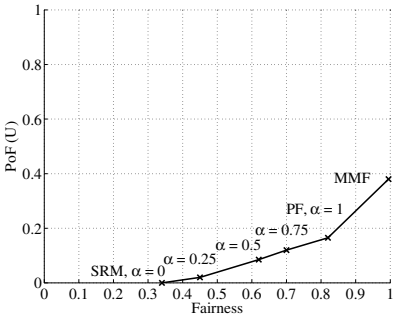

Fig. 1. The trade-off between efficiency and fairness is depicted for a family of utility functions.

B. Contributions

In this paper, we study the FDPS problem in an SC-FDMA system. We follow the optimal solution framework in [8], but employ it with RB granularity in the frequency domain to reduce computational complexity by two orders of magnitude. Our solution approach involves a utility-based resource allocation scheme such that we can exploit the multiuser diversity. We formulate the FDPS problem as a set partitioning problem which can be solved by branch-and-cut methods. We investigate a family of utility functions called as the α-fair utility function. In particular, we study the SRM, PF, and max-min fair (MMF) utilities. We consider the functions of user capacity as the utility to be maximized,

and define the system efficiency as the sum of user rates. By using these utility functions, we solve the FDPS problem. We identify the optimality conditions, and present the size of the solution spaces and computational complexities of these schedulers. Moreover, we propose to use the price of fairness as a comparison metric between schedulers. The price of fairness of a scheduler defines the amount of aggregate loss of a scheduler when compared to the SRM scheduler. Along with a fairness index (such as Jain's fairness index [21]), the decision maker can acquire how much system efficiency loss is incurred while improving fairness by a certain amount. To the best of our knowledge, this metric has not been explored in a multiuser cellular radio environment. We depict the trade-offs between efficiency and fairness for α-fair schedulers in Fig. 1. The SRM scheduler achieves the highest system efficiency of 1, i.e., the price of fairness of SRM scheduler is 0, but it lacks fairness among the users. When fairness is introduced to the system, the system efficiency decreases, or equivalently, the price of fairness increases. At the highest fairness, MMF scheduler maximizes the minimum user rate. Unfortunately, the $(1, 0)$ point on Fig. 1 cannot be achieved since the most efficient solution lacks fairness, and the most fair solution lacks efficiency. Also, note that these points correspond to the optimal scheduler solutions that are Pareto optimal which means that there is no user whose rate can be increased without decreasing the rates of other users. With the use of price of fairness metric, this paper answers the following questions: How do the cell-edge users get affected when the scheduler tries to maximize the sum-rate per cell? How can we improve fairness among users, especially between cell-center and cell-edge users? And, how much aggregate rate loss is incurred while introducing fairness? We present upper bounds on the aggregate cell rate loss for the PF scheduler. We describe how to include DFT constraints to construct RB assignment patterns and how to form the constraint matrix. The optimality conditions of the investigated problems are also presented. The analytical framework is supported with the numerical results of these FDPS problems. We derive conclusions based on the trade-offs between different types of schedulers.

The remainder of this paper is organized as follows. Section II introduces the system model and discusses the uplink power control in LTE systems. Section III presents the utility-based resource allocation framework and discusses α-fair utility functions. Also, we define and provide the upper bounds on the price of fairness in this section to quantify the scheduler efficiencies. In Section IV, we study and formulate the scheduling problems. We identify the necessary optimality conditions for the α-fair schedulers. An effective solution method is also presented. The implementation constraints and exact dimensions of the search spaces are also investigated. Sections V-VI discuss the results of proposed FDPS problems in a realistic simulation environment along with some concluding remarks.

II. System Model

In this section, SC-FDMA uplink system model and the uplink power control mechanism in LTE standards are described. First, we start with introducing the notations used in this paper. The vectors and matrices are represented by boldface characters, e.g., $\mathbf{x}$, $\mathbf{A}$. The dimensions of the vectors are shown by subscripts, e.g., $\mathbf{x}_N$ is an $N \times 1$ column vector. Vectors in a set are enumerated by superscripts, e.g., $\mathbf{x}_N^1, \ldots, \mathbf{x}_N^K$. We use $\mathbf{1}_N$ and $\mathbf{0}_N$ to denote all ones and all zeros column vectors, respectively. The transpose of a column vector $\mathbf{x}$ is given by $\mathbf{x}^T$. The sets are shown by capital calligraphic font, e.g., the set $\mathcal{N}$ includes $\mathcal{N} = \{1, \ldots, N\}$. A subset of set $\mathcal{N}$ is denoted by subscripting it as $\mathcal{N}_k$, and $|\mathcal{N}_k|$ denotes the cardinality of the subset. The total number of ones in vector $\mathbf{x}$ is denoted by $\mathbf{w}(\mathbf{x})$ where $\mathbf{x}$ consists of binary elements 0 and 1. Finally, any power value P is represented in dB with the notation P^{dB}.

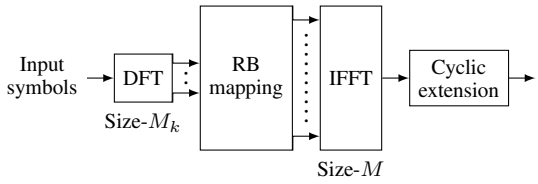

Fig. 2. The transmitter structure of an SC-FDMA system.

Assume that the system bandwidth consists of M orthogonal subcarriers. These subcarriers can be grouped into clusters to form N non-overlapping RBs. For example, according to LTE specifications, a system with 10 MHz bandwidth occupies $M = 600$ subcarriers, or equivalently, $N = 50$ RBs, and each RB consists of $N_{sc}^{RB} = 12$ consecutive subcarriers [2]. Let the total set of subcarriers and RBs be denoted by $\mathcal{M}$ and $\mathcal{N}$, respectively. Then, $\mathcal{M}_k$ and $\mathcal{N}_k$ represent the set of subcarriers and RBs assigned to user k, respectively. Also, the complete set of users in the system is represented as $\mathcal{K} = \{1, \ldots, K\}$, and those associated with base station c are given by the subset $\mathcal{K}_c$. The cardinality of this subset, $K_c = |\mathcal{K}_c|$, denotes the total number of users associated with base station c. When all the RBs in the system are scheduled, $N = |\mathcal{N}| = M/N_{sc}^{RB} = |\mathcal{N}_1| + \cdots + |\mathcal{N}_{K_c}| = N_1 + \cdots + N_{K_c}$ holds true. Furthermore, let $\mathcal{K}_m$ denote the set of users that are assigned to subcarrier m, and note that the set of users in $\mathcal{K}_m$ are located in different cells in a multi-cell multiuser scenario.

The transmitter structure of an uplink SC-FDMA system is depicted in Fig. 2. It includes DFT, subcarrier mapping, and inverse fast Fourier Transform (IFFT) operations. In LTE systems, due to the orthogonal resource assignments in time, frequency and spatial domains help avoid the near-far problems that existed in Wideband Code Division Multiple Access (WCDMA). For this reason, power control in LTE is carried out at a slower rate [2]. For a given user-base station assignment, the fractional open-loop power control is expressed as [22]

$$P_k^{dB} = \min\{P_{\max}^{dB}, P_0^{dB} + 10\log_{10}(N_k) + \beta PL_{k,c_k}^{dB}\}, \quad (1)$$

where P_k^{dB} denotes the uplink transmit power of user k, and $P_{\max}^{dB}$ denotes the maximum UE transmit power. P_0^{dB} is the open loop transmit power. PL_{k,c_k}^{dB} is the path loss between user k and its serving base station c_k. We consider that the path loss includes the shadow fading of the link. Since shadow fading is a slow variation process for pedestrian speeds, we assume it to be static over a frame duration [15].

The path loss compensation factor β takes its value from the set $\{0,0.4,0.5,0.6,0.7,0.8,0.9,1\}$. It determines the fairness within the cell such that the network enables cell-edge users with high path loss values to transmit at high power levels for $\beta = 1$. The fairness in the system decreases as the path loss compensation approaches zero, i.e., $\beta \to 0$, since the high path losses for cell-edge users are not compensated for. However, this improves the rates for the cell-center and median users due to reduced intercell interference compared to the full path loss compensation case. The UE transmission power is equally distributed on the allocated bandwidth such that the UE transmit power per subcarrier is $P_{k,m} = P_k/M_k$ in linear scale.

Furthermore, in order to investigate the performance of the frequency-domain scheduler, frequency selective fading channel models are considered. For example, [14] provides power delay profile models for pedestrian and vehicular users. We denote the channel gain between user k and base station c on subcarrier m by $H_{k,c}(m)$. The channel gain has two components, consisting of multipath and path loss plus shadowing components. They can be expressed as

$$H_{k,c}(m) = \frac{|V_{k,c}(m)|^2}{PL_{k,c}},\ V_{k,c}(m) = \sum_{l=1}^{L} v_k(l) \exp\left(\frac{-j2\pi m \tau_l}{T_s}\right), \tag{2}$$

where $V_{k,c}(m)$ includes the multipath effects in the received signal for an L-path impulse response model. T_s and τ_l denote the sampling time and the delay of l-th path, respectively. Each multipath component $v_k(l)$ can be further expressed as

$$v_k(l) = \begin{cases} A\sqrt{P_{rel}(l)}w_k(l) & \text{if } \ l = \lfloor \tau_l/T_s \rfloor + 1 \\ 0 & \text{otherwise,} \end{cases} \tag{3}$$

where $w_k(l)$ denotes a zero-mean Gaussian noise process. $P_{rel}(l)$ denotes the relative power of the l-th path. The term A normalizes the average multipath power to unity such that $E[\sum |v_k(l)|^2] = 1$. The sampling time T_s and the sampling frequency f_s in LTE systems depend on the system bandwidth. The sampling frequency is given by $f_s = 1/T_s = B_{sc}M$, where the total number of subcarriers M is also the IFFT size and the bandwidth of each subcarrier is fixed to $B_{sc} = 15$ kHz. For example, in a 10 MHz bandwidth, there are 600 subcarriers and $M = 1024$. Then, the sampling frequency becomes $f_s = 15.36$ MHz [23, p. 70]. The SNR on each subcarrier m assigned to user k is given by

$$\gamma_{k,m} = \frac{P_{k,m}H_{k,c}(m)}{\sigma_c^2} = \frac{P_{k,m}|V_{k,c}(m)|^2}{PL_{k,c}\,\sigma_c^2}, \tag{4}$$

where σ_c^2 is the thermal noise effective on a subcarrier at base station c. Similarly, the signal-to-interference-plus-noise ratio (SINR) of user k on subcarrier m is given by

$$\Gamma_{k,m} = \frac{P_{k,m}H_{k,c}(m)}{\sum_{j\in\mathcal{K}_m, j\neq k} P_{j,m}H_{j,c}(m) + \sigma_c^2}. \tag{5}$$

We assume that ideal channel estimates for each link are available. Typically, frequency domain minimum mean square error (MMSE) equalizers are employed at the base station receivers. The wideband SNR for user k, γ_k, can be calculated using the individual SNR of each subcarrier m assigned to user k, $\gamma_{k,m}$ as [23], [24]

$$\gamma_k = \left(\frac{1}{\frac{1}{M_k}\sum\limits_{m\in\mathcal{M}_k}\frac{\gamma_{k,m}}{\gamma_{k,m}+1}} - 1\right)^{-1}. \tag{6}$$

Similarly, the wideband SINR of user k, Γ_k, can be defined by replacing $\gamma_{k,m}$ with $\Gamma_{k,m}$ in (6). The channel capacity of user k defines the maximum reliable communication rate over a channel. However, in practical communication systems, one needs to account for other factors (e.g., reference signals, control signal overhead, frame retransmissions, etc.) to derive the actual throughput of a user. Therefore, the throughput of a user depends on the system parameters and protocols. It is shown in [25] that these factors can be accounted for by scaling the bandwidth and the SINR such that the throughput of user k is given by

$$C_k(\Gamma) = b_1 B_{sc} N_k N_{sc} \log_2\left(1 + \Gamma_k/b_2\right), \tag{7}$$

where b_1 accounts for the bandwidth losses due to control signals and b_2 considers the SINR implementation efficiency of LTE. However, in a multi-cell scenario, estimating the exact interference levels per subframe requires excessive traffic signaling among base stations. Therefore, in this paper, we use the throughput estimates based on the SNR of each link during scheduling phase. This corresponds to noncooperative scheduling in game theory [26]. Hence, the scheduler at each base station uses the following utility

$$C_k(\gamma) = b_1 B_{sc} N_k N_{sc} \log_2\left(1 + \gamma_k/b_2\right), \tag{8}$$

to solve the FDPS problem. The same type of scheduling is also studied in [7]–[13], [16]–[18].

III. Utility-Based Resource Allocation

In this section, we present the utility-based resource allocation and study a family of utility functions that enable us to investigate the SRM, PF, and MMF schedulers. We also discuss the price of fairness metric and investigate the corresponding upper bounds for each of these schedulers.

A. Utility Functions

To analyze the utility-based frequency-domain resource allocation in noncooperative cells, we use the α-fair utility function that is defined in [27] as

$$U_\alpha(C_k) = \begin{cases} \log(C_k) & \text{if } \alpha = 1 \\ C_k^{1-\alpha}/(1-\alpha) & \text{if } \alpha \neq 1, \alpha \geq 0, \end{cases} \tag{9}$$

where α is the parameter that characterizes the efficiency and fairness trade-off. When $\alpha = 0$ is considered, the scheduler simply maximizes the sum of individual utilities. This is also called as the utilitarian solution in optimization theory and it has the maximum efficiency [3]. In this paper, we refer to this allocation as the SRM scheduler. In cellular radio systems, this corresponds to the best effort solution.

When $\alpha = 1$, the scheduler is referred to as the PF scheduler. This scheduler is well-studied in the literature [3], [4], [27]–[29].

$$\sum_{k=1}^{K_c} \frac{r_k - r_k^*}{r_k^*} \leq 0, \tag{10}$$

where r_k and r_k^* are the kth elements of the rate vectors $\mathbf{r}$ and $\mathbf{r}^*$, respectively.

In general, as α increases, the efficiency of the system decreases [3], [4] (see [30] for a unique counter example). The MMF scheduler maximizes the minimum rate offered to the users and achieves the maximum fairness. Besides the SRM, PF, and MMF schedulers, we will also look into α values in the range $0 < \alpha < 1$ to further analyze the trade-offs between efficiency and fairness.

In order to provide the reader some intuition about utility functions, the following observations are important. Notice that the α-fair utility function in (9) is a nondecreasing concave up function for $\alpha > 0$. This makes this utility function achieve fairness as α increases. This can be shown as follows. We know that if $U_\alpha(C)$ is a nondecreasing concave up function, then $U'_\alpha(C_k) \geq U'_\alpha(C_j)$ for $C_k \leq C_j$, where $U'_\alpha(C)$ denotes the derivative of the utility function. This means that for any nondecreasing concave up utility function, the increases in small rates are more favored compared to the larger rates. Note that we are using the terms rate and utility interchangeably since we focus on the user rate as the utility to be maximized. Similarly, any nondecreasing convex (concave down) utility function that one defines will favor the increases in the larger utilities. When the utility function is linear, the increases in all utilities are favored equal.

B. The Price of Fairness

We can now introduce the price of fairness as a metric to compare scheduler efficiencies. When resources are shared among users, natural questions on how to allocate resources and how to balance the trade-off of efficiency versus fairness arise. In fact, this general problem can be observed in many areas of economics, finance, and social welfare. In the sequel, we define the expressions for the price of fairness and derive the upper bounds in both single-cell and multi-cell environments. In particular, the detrimental effects of interference need to be considered in the multi-cell scenario. Let us first start with defining the system efficiency of the SRM scheduler in a single-cell scenario as

$$U_{SRM}(\gamma) = \sum_{k \in \mathcal{K}_c} C_k^*(\gamma), \tag{11}$$

where $C_k^*(\gamma)$ represents the throughput of users associated with base station c in the optimal solution. Similarly, the aggregate throughput of the optimal solutions for the α-fair, PF, and MMF schedulers are denoted by U_α, U_{PF}, and U_{MMF}, respectively. Next, the price of fairness is defined as the percentage loss in the efficiency of a scheduler when compared to the utilitarian solution [3], [4]. In a single-cell scenario, it is given by

$$\mathrm{PoF}\left(U(\gamma)\right) = \frac{U_{SRM}(\gamma) - U(\gamma)}{U_{SRM}(\gamma)}, \tag{12}$$

where $U(\gamma)$ denotes the sum of utilities for any scheduler, and $\mathrm{PoF}\left(U(\gamma)\right)$ ranges between 0 and 1. A lower price of fairness means higher efficiency. It achieves its lowest value of zero at the utilitarian solution, i.e., $U = U_{SRM}$. In general, as the system efficiency decreases, fairness in the system increases, and consequently, the price of fairness increases. At the worst case, when the scheduler does not schedule any resources, the price of fairness becomes 1.

The application of this metric in wireless cellular radio communications enables us to quantify the performance of different schedulers and select the parameter α. Let us note that in cellular radio communications, each user experiences different channel conditions due to the random nature of wireless radio. Therefore, they have different maximum achievable utilities. For instance, cell-center users achieve significantly higher peak rates compared to those of cell-edge users. In [4], upper bounds are derived for the price of fairness of α-fair schedulers where users have unequal achievable utilities. They are given by

$$\mathrm{PoF}(U_\alpha) \leq 1 - \min_{x \in [1, K_c]} \frac{\left(\frac{B}{L}\right)^{\frac{1}{\alpha}} x^{1+\frac{1}{\alpha}} + K_c - x}{\left(\frac{B}{L}\right)^{\frac{1}{\alpha}} x^{1+\frac{1}{\alpha}} + \frac{B}{L}(K_c - x)x}, \tag{13}$$

where B and L represent the highest and lowest maximum achievable utilities over all users, respectively. In order to find appropriate B and L parameters, we make the following observation. In an adaptive bandwidth system, the maximum achievable utility of user k is achieved when full bandwidth is scheduled to user k. Then, B and L are given as

$$B = b_1 B_{sc} M \log_2\left(1 + \frac{\gamma_l}{b_2}\right), \text{ s.t. } l = \arg\max_{k \in \mathcal{K}_c} C_k(\gamma) \tag{14}$$

$$L = b_1 B_{sc} M \log_2\left(1 + \frac{\gamma_m}{b_2}\right), \text{ s.t. } m = \arg\min_{k \in \mathcal{K}_c} C_k(\gamma),$$

where γ_l and γ_m denote the wideband SNR values when the whole bandwidth is scheduled to users l and m, respectively. As the ratio of the highest to lowest maximum achievable utility, B/L, increases, the bound in (13) loosens [4]. Similarly, the price of fairness in a multi-cell scenario is defined as

$$\mathrm{PoF}\left(U(\Gamma)\right) = \frac{U_{SRM}(\Gamma) - U(\Gamma)}{U_{SRM}(\Gamma)}, \tag{15}$$

where $U_{SRM}(\Gamma)$ and $U(\Gamma)$ denote the sum of user throughput including the interference such as $U(\Gamma) = \sum_{k \in \mathcal{K}_c} C_k(\Gamma)$. In Section V, we demonstrate that employing this metric and the bounds on each α-fair scheduler give network operators an analytical tool to compare and quantify the efficiency and fairness trade-offs.

C. A Case Study

Consider a network where the SRM scheduler satisfies the QoS constraints of users and the network operator wants to increase the fairness in the network without violating these constraints. Let us assume that the network operator can tolerate a system efficiency loss up to 20% compared to the SRM scheduler in order to increase the fairness and we want to determine an appropriate α value such that the efficiency and fairness trade-off can be balanced. This scenario may occur in cases where the operators need to improve the user satisfaction

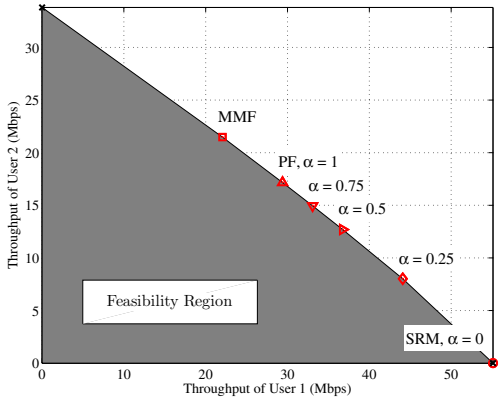

Fig. 3. Feasibility region is depicted for a single-cell network with $K_c = 2$ users and $N = 15$ RBs.

considering the QoS constraints. In this example, we consider a simplified simulation setup with $K_c = 2$ users and $N = 15$ RBs in a single-cell scenario. Fig. 3 depicts the feasibility region for different α values. We identify the critical points in the feasibility region that correspond to optimal solutions of different α-fair schedulers. Note that the boundaries of the feasibility region are Pareto optimal, which was discussed in Section I-B. We assume that $P_0^{dB} = -70$ dBm and $\beta = 1$ is employed. Furthermore, let the path loss values of user 1 and 2 to be 60 dB and 90 dB, respectively, and ignore the frequency fading and shadow fading for the sake of simplicity. The corresponding solutions and the feasibility region are depicted in Fig. 3. It can be observed that the SRM scheduler maximizes the sum rate without any fairness concerns. It assigns all the resources to user 1 which achieves 55.11 Mbps, while user 2 is not served. The PF scheduler ignores the solution where any user is not assigned any resources since the payoff of such a solution will be $\log(0) = -\infty$. Instead, the PF scheduler always allocates a resource to each user and achieves a more fair distribution of resources compared to the SRM scheduler. In this case, it assigns 8 RBs and 7 RBs to users 1 and 2, respectively, and their throughput are 29.39 Mbps and 17.16 Mbps. It can be observed that as the fairness is introduced to the system, the system efficiency is reduced. Also, we observe that the MMF scheduler allocates more RBs to the users with low channel gains in order to increase the minimum rate user. This is achieved, again, at the expense of system efficiency. With the MMF scheduler, users 1 and 2 are assigned 6 RBs and 9 RBs, respectively, and they are served at 22.05 Mbps and 21.48 Mbps.

The maximum achievable utilities of users 1 and 2 are 55.1 Mbps and 33.8 Mbps, respectively. The theoretical upper bounds of the price of fairness for $\alpha = \{0.25, 0.5, 0.75, 1\}$ and the MMF scheduler are $\{0.073, 0.147, 0.179, 0.199, 0.282\}$, respectively, using the bounds in (13). The empirical values of the price of fairness are $\{0.055, 0.103, 0.129, 0.155, 0.210\}$, in the same order as before. Notice that the bounds are tight. Also, for the given system efficiency tolerance, the network operator decides to employ $\alpha = 1$ by only using the maximum achievable utilities of its users without the need of extensive simulations.

IV. FDPS Schedulers

In this section, we present the FDPS problem formulation, implementation constraints, optimality conditions, set partitioning method, and solution space dimensions.

A. Problem Formulation

We can now discuss the uplink FDPS problem for an SC-FDMA system. As shown earlier, we investigate a family of objectives parameterized by a single variable, α. Given the utility function defined in (9), the FDPS problem can be mathematically expressed as follows

$$\textbf{P1:} \quad \max_{\{\mathcal{N}_1,\ldots,\mathcal{N}_{K_c}\}\in\mathcal{N}} \sum_{k=1}^{K_c} \omega_k U_\alpha\left(C_k(\gamma)\right) \tag{16a}$$

$$\text{s.t.} \quad \mathcal{N}_k \cap \mathcal{N}_j = \emptyset, \ \forall k \neq j \tag{16b}$$

$$\mathcal{N}_1 \cup \cdots \cup \mathcal{N}_{K_c} \subseteq \mathcal{N} \tag{16c}$$

$$N_k \in \{1, \ldots, N\}, \ \forall k \tag{16d}$$

where ω_k denotes the nonnegative QoS weight for user k. The first constraint assigns each RB to only one user without any overlap, and the second constraint ensures that all the resources are assigned. The third constraint denotes that the cardinality of the set of RBs scheduled to user k can take any integer values up to N. Note that the construction of RB assignment sets, $\mathcal{N}_k$, ensures the contiguity of RB assignments.

In a multiuser scenario, there may exist assignments that yield cases where some users do not get any resources. We refer to this as the user rate starvation, and it creates a significant problem for network operators in terms of satisfying user experience and QoS requirements. Typically, user rate starvation occurs when the cell-edge users that experience low channel gains are not served at the benefit of improving the rates of cell-center users. In order to avoid user rate starvation cases, we consider the following assumption.

Assumption 1: At every subframe, each user $k \in \mathcal{K}_c$, connected to base station c_k, is assigned at least one RB.

Assumption 1 can be incorporated into problem P1 by introducing an additional constraint. Then, we rewrite the scheduling problem as

$$\textbf{P2:} \quad \max_{\{\mathcal{N}_1,\ldots,\mathcal{N}_{K_c}\}\in\mathcal{N}} \sum_{k=1}^{K_c} \omega_k U_\alpha\left(C_k(\gamma)\right) \tag{17a}$$

$$\text{s.t.} \quad \mathcal{N}_k \cap \mathcal{N}_j = \emptyset, \ \forall k \neq j \tag{17b}$$

$$\mathcal{N}_1 \cup \cdots \cup \mathcal{N}_{K_c} \subseteq \mathcal{N} \tag{17c}$$

$$1 \leq N_k \leq N - K_c + 1, \forall k \in \mathcal{K}_c \tag{17d}$$

where the third constraint includes Assumption 1. We use P2 to solve the PF scheduling problem efficiently. Section IV-E discusses that this constraint significantly reduces the search space and results in a faster algorithm. Note that for the PF scheduler, any user that does not get any resources contributes to the objective as $\log(0) = -\infty$, and the optimal solution does not allow such an allocation.

The MMF scheduling problem considers the same constraints in P2 but it has a different objective. This problem

can be written as

$$\textbf{P3:} \max_{\{\mathcal{N}_1,\ldots,\mathcal{N}_{K_c}\}\in\mathcal{N}} \min_{k\in\mathcal{K}_c} \omega_k U_\alpha\left(C_k(\gamma)\right) \quad (18a)$$
$$\text{s.t.} \quad (17b)-(17d).$$

If a user is not allocated any resource, then the objective of the MMF scheduler will be zero which does not occur unless $K_c > N$, and we avoid this condition in this paper. Hence, using P2-P3 instead of P1 for the PF and MMF schedulers still achieves the optimal solution when $K_c \leq N$ is satisfied.

B. Implementation Constraints

The practical constraints for the SC-FDMA system include those of the DFT implementations. In order to support an efficient DFT design, it was agreed in [31] to restrict the largest prime-factor that needs to be supported. In this paper, we consider the implementation of radix set $\{2, 3, 5\}$. Then, the number of RBs assigned to a user needs to be divisible by 2, 3, and 5. Note that, although we have only considered these three radices for a computationally fast implementation, this can be extended to include any radices. Hence, the number of resources allocated to user k in the uplink can only take the following values [32, p. 17] [23],

$$N_k = |\mathcal{N}_k| = 2^{\upsilon_1} \times 3^{\upsilon_2} \times 5^{\upsilon_3},\ \forall\ k \in \mathcal{K}_c \quad (19)$$

where υ_1, υ_2, and υ_3 are non-negative integers. It is shown in [31] that the DFT constraints of the above radix set reduce the number of complex multiplications more than five-folds compared to the unconstrained case.

The DFT constraints can be added to the FDPS problem as follows

$$\textbf{P4:} \max_{\{\mathcal{N}_1,\ldots,\mathcal{N}_{K_c}\}\in\mathcal{N}} \sum_{k=1}^{K_c} \omega_k U_\alpha\left(C_k(\gamma)\right) \quad (20a)$$
$$\text{s.t.} \quad \mathcal{N}_k \cap \mathcal{N}_j = \emptyset,\ \forall\, k \neq j \quad (20b)$$
$$\mathcal{N}_1 \cup \cdots \cup \mathcal{N}_{K_c} \subseteq \mathcal{N} \quad (20c)$$
$$N_k = 2^{\upsilon_1}\, 3^{\upsilon_2}\, 5^{\upsilon_3},\ \forall\, k \in \mathcal{K}_c \quad (20d)$$
$$1 \leq N_k \leq N - K_c + 1,\ \forall k \in \mathcal{K}_c \quad (20e)$$

where the constraint in (20d) includes the DFT constraint that the number of RBs that can be scheduled to a user needs to be a multiple of the radix set. The last constraint in (20e) ensures that every user gets at least one RB. Section V discusses the simulation results with and without the DFT constraints in order to observe the effects of implementation constraints on the system efficiencies.

C. Optimality Conditions

Let $\mathcal{U}$ denote the set of feasible throughput vectors. Suppose $\mathbf{r}, \mathbf{r}^* \in \mathcal{U}$ denote two feasible rate vectors, then $\mathbf{r}^*$ is optimal if it satisfies the first-order optimality condition, that is,

$$\nabla U_\alpha\left(\mathbf{r}^*\right)\left(\mathbf{r}-\mathbf{r}^*\right) = \sum_{k=1}^{K_c} \frac{\left(r_k - r_k^*\right)}{\left(r_k^*\right)^\alpha} \leq 0,\ \forall\, \mathbf{r} \in \mathcal{U} \quad (21)$$

where $\nabla U_\alpha\left(\cdot\right)$ denotes the derivative of the utility function with respect to C_k and for $\alpha \geq 0$ [33]. In the special case, when $\alpha = 1$, then (21) satisfies the proportional fairness condition in (10). The optimality condition in (21) can be rewritten as

$$\mathbf{g}^T\mathbf{r} \leq 1,\ \forall\, \mathbf{r} \in \mathcal{U} \quad (22)$$

where the elements of $\mathbf{g}$ are given by

$$g_k = \frac{\left(r_k^*\right)^{-\alpha}}{\sum_{k=1}^{K} \left(r_k^*\right)^{1-\alpha}},\ \forall\, k \in \mathcal{K}_c. \quad (23)$$

Moreover, since the α-fair utility function is twice differentiable, the second-order sufficiency condition for $\mathbf{r}^*$ is that

$$\left(\mathbf{r}-\mathbf{r}^*\right)^T \nabla^2 U_\alpha(\mathbf{r}^*)\left(\mathbf{r}-\mathbf{r}^*\right) = -\alpha \sum_{k=1}^{K_c} \frac{\left(r_k - r_k^*\right)^2}{\left(r_k^*\right)^{1+\alpha}} < 0 \quad (24)$$

is satisfied for all $\mathbf{r} \in \mathcal{U}$, $\mathbf{r} \neq \mathbf{r}^*$, where $\nabla^2 U_\alpha(\cdot)$ denotes the Hessian matrix of the utility function [33].

D. Set Partitioning Solution

The problems investigated above can be cast as binary integer programming problems. The following special form is referred to as the set partitioning problem [34]

$$\max_{\mathbf{x}} \ \mathbf{f}^T\mathbf{x} \quad (25)$$
$$\text{s.t.}\ \ \mathbf{A}\mathbf{x} = \mathbf{1},\ \ x_i \in \{0,1\},\ \forall\, i$$

where $\mathbf{A}$ denotes the constraint matrix with binary elements 0 and 1. The vectors $\mathbf{f}$ and $\mathbf{x}$ are the weighting and the binary assignment vectors, respectively. Both vectors have dimension $JK_c \times 1$, where J denotes the total number of possible contiguous resource allocation patterns for each user, and it will be further explained in the sequel. The binary variable $x_{jk} \in \mathbf{x}$ is associated with RB assignment pattern j for user k. We assign $x_{jk} = 1$ if RB assignment pattern j is assigned to user k, and 0 if not. Only one RB assignment pattern, corresponding to a column of $\mathbf{A}$, can be selected per user.

The objective vector $\mathbf{f}$ requires constant channel state information (CSI) updates per subframe in order to adapt to the varying channel conditions. The α-fair utility function for $0 \leq \alpha < 1$ uses the following objective function

$$f_{k,m} = \sum_{m\in\mathcal{M}_k} \omega_k \frac{\left(b_1 B_{sc} N_k N_{sc}^{RB} \log_2\left(1+\gamma_k/b_2\right)\right)^{1-\alpha}}{1-\alpha}. \quad (26)$$

In the special case, when $\alpha = 0$, the SRM scheduler maximizes the aggregate throughput. Similarly, the objective function for the PF scheduler is

$$f_{k,m} = \sum_{m\in\mathcal{M}_k} w_k \log\left(b_1 B_{sc} N_k N_{sc}^{RB} \log_2\left(1+\gamma_k/b_2\right)\right) \quad (27)$$

where the objective is to maximize the sum of the logarithm of utilities. Note that the base of the logarithm operator is not critical. Unlike previous schedulers, an auxiliary variable ν needs to be introduced to solve the MMF scheduler. Then,

using the auxiliary variable, the MMF scheduler problem can be translated into a mixed integer program such that

$$\begin{aligned} \max_{\mathbf{x}} \ & \nu \\ \text{s.t. } & \nu \leq \mathbf{f}^T\mathbf{x} \\ & \mathbf{A}\mathbf{x} = \mathbf{1}, \ \ x_i \in \{0,1\}, \forall\, i \end{aligned} \tag{28}$$

where ν is a free variable and $\mathbf{f}$ is given in (26) with $\alpha = 0$.

The constraint matrix $\mathbf{A}$ is created once, and does not require any updates as long as the number of users connected to the base station stays the same. The matrix $\mathbf{A}$ has dimension $(K_c + N) \times JK_c$, and it can be expressed as

$$\mathbf{A} = \left[\begin{array}{cccc} \mathbf{A}_1 & \mathbf{A}_2 & \cdots & \mathbf{A}_{K_c} \\ \mathbf{1}_J^T & \mathbf{0}_J^T & \cdots & \mathbf{0}_J^T \\ \mathbf{0}_J^T & \mathbf{1}_J^T & \ddots & \vdots \\ \vdots & \ddots & \ddots & \mathbf{0}_J^T \\ \mathbf{0}_J^T \cdots & & \mathbf{0}_J^T & \mathbf{1}_J^T \end{array}\right], \tag{29}$$

where each submatrix $\mathbf{A}_k$ has dimension $N \times J$. For illustration purposes, the constraint matrix $\mathbf{A}$ is divided into two parts in (29). The upper portion of $\mathbf{A}$ is composed of concatenation of submatrices, $[\mathbf{A}_1, \ldots, \mathbf{A}_{K_c}]$. Without loss of generality, we consider that $\mathbf{A}_k$'s are the same for each user. Also, each submatrix, $\mathbf{A}_k$ represents the set of all RB assignment patterns with the contiguity constraint, and it can be written as

$$\mathbf{A}_k = \left[\ \mathbf{q}_N^1, \ldots, \mathbf{q}_N^J\ \right], \forall k \in \mathcal{K}_c \tag{30}$$

where each column of $\mathbf{A}_k$, that is $\mathbf{q}_N^j, j \in \{1, \ldots, J\}$ represents one possible contiguous RB assignment pattern. For example, the binary vector $\mathbf{q}_N^1 = [1, 0, \ldots, 0]^T$ assigns the first RB to user k. Also, notice that the weight of the assignment pattern, $\mathbf{w}(\mathbf{q}_N^j)$, is equal to the cardinality of RB assignment set $|\mathcal{N}_k|$, that is N_k, and we express this as $\mathbf{w}(\mathbf{q}_N^j) = |\mathcal{N}_k| = N_k$, $\forall k \in \mathcal{K}_c$. Lower portion of the constraint matrix $\mathbf{A}$ in (29) has K_c rows, and it ensures that each user is assigned only one RB assignment pattern. For this purpose, it is structured in a staircase form where each row of $\mathbf{A}_k$ has J consecutive entries of ones and each column has only a single one entry. The remaining entries of $\mathbf{A}_k$ are all zeros. In fact, the construction of the constraint matrix $\mathbf{A}$ with the contiguity constraint is what distinguishes single carrier localized-FDMA schedulers from OFDM schedulers. As an example, assume that $N = 4$ RBs and $M = 2$ users. Then, the constraint submatrix $\mathbf{A}_k$ for problem P1 is given by

$$\mathbf{A}_k = \left[\begin{array}{cccccccccccc} 0 & 1 & 0 & 0 & 0 & 1 & 0 & 0 & 1 & 0 & 1 \\ 0 & 0 & 1 & 0 & 0 & 1 & 1 & 0 & 1 & 1 & 1 \\ 0 & 0 & 0 & 1 & 0 & 0 & 1 & 1 & 1 & 1 & 1 \\ 0 & 0 & 0 & 0 & 1 & 0 & 0 & 1 & 0 & 1 & 1 \end{array}\right] \tag{31}$$

where the columns of $\mathbf{A}_k$ correspond to RB assignment patterns, $\mathbf{q}_N^j, j \in \{1, \ldots, J\}$, with $J = 11$. When we impose Assumption 1, then the first and last columns of $\mathbf{A}_k$ in (31) need to be removed. The DFT constraints can be included to the constraint submatrix $\mathbf{A}_k$ for P3 by removing the columns that does not satisfy $\mathbf{w}(\mathbf{q}_N^j) = |\mathcal{N}_k| = 2^{\upsilon_1}3^{\upsilon_2}5^{\upsilon_3}$. Then, the constraint submatrix for P2 and P3 are

$$\mathbf{A}_k = \left[\begin{array}{ccccccccc} 1 & 0 & 0 & 0 & 1 & 0 & 0 & 1 & 0 \\ 0 & 1 & 0 & 0 & 1 & 1 & 0 & 1 & 1 \\ 0 & 0 & 1 & 0 & 0 & 1 & 1 & 1 & 1 \\ 0 & 0 & 0 & 1 & 0 & 0 & 1 & 0 & 1 \end{array}\right] \tag{32}$$

where $J = 9$. In the next section, we shall present, in detail, how to find the total number of resource allocation patterns for each of the above problems.

E. Finding The Exact Search Spaces

Now, we can discuss the total number of resource allocation patterns for the problems P1-P4 when the set partitioning approach is applied. First, let us consider the FDPS problem in P1. The total number of RB allocation patterns for the SRM scheduler is

$$J_1 = 1 + \sum_{i=1}^{N} (N - (i-1)) = \frac{N^2}{2} + \frac{N}{2} + 1 \tag{33}$$

where $N \geq K_c$, and J_1 increases as the number of RBs increase. Note that J_1 is independent of the number of users in the system.

Next, we look at the total number of RB assignment patterns for P2. This case corresponds to the PF and MMF schedulers, and it includes Assumption 1. Then, the total number of RB allocation patterns is given by

$$J_2 = \sum_{i=1}^{N-K_c+1} (N - (i-1)) = (N - K_c + 1)\left(\frac{N}{2} + \frac{K_c}{2}\right) \tag{34}$$

where $N \geq K_c$. Also, in order to investigate the effects of DFT implementation constraints, we revisit the SRM, PF, and MMF scheduling problems. When we impose the DFT constraints for the SRM scheduler, the total number of RB allocation patterns is

$$J_3 = \frac{N^2}{2} + \frac{N}{2} + 1 - \sum_{i \in \mathcal{E}_1} (N - (i-1)) \tag{35}$$

where the set $\mathcal{E}_1$ denotes the set of numbers that cannot be achieved using the powers of radix set. An example set is $\mathcal{E}_1 = \{7, 11, 13, 17, 19, \ldots\}$. Note that the largest element in $\mathcal{E}_1$ can be at most N. Similarly, when we consider Assumption 1 and the DFT constraints, the total number of RB allocation patterns for the PF and MMF schedulers become

$$\begin{aligned} J_4 &= \sum_{i=1}^{N-K_c+1} (N - (i-1)) - \sum_{i \in \mathcal{E}_2} (N - (i-1)) \\ &= (N - K_c + 1)(N/2 + K_c/2) - \sum_{i \in \mathcal{E}_2} (N - (i-1)) \end{aligned} \tag{36}$$

where $N \geq K_c$. $\mathcal{E}_2$ includes the set of numbers that are not multiples of the radix set. The largest element of $\mathcal{E}_2$ is at most equal to $N - K_c + 1$ due to Assumption 1.

As a final remark, if this resource allocation problem is solved with subcarrier granularity instead of RB granularity,

the total number of subcarrier assignment patterns per user becomes

$$J_5 = 1 + \sum_{i=1}^{M} M - (i-1) = \frac{M^2}{2} + \frac{M}{2} + 1 \qquad (37)$$

where $M \geq K_c$. Obviously, resource allocation pattern size with subcarrier granularity in (37) is prohibitively complex to be implemented in real time.

In order to give the reader a sense of the dimensions of the problems investigated in this paper, we give an example assignment in an LTE system. Assume a bandwidth of 10 MHz with 50 RBs, and 12 users per sector, J_1, J_2, J_3, J_4, and J_5 are 1276, 1209, 739, 717, and 180301, respectively. Since the problem size closely depends on the total number of RB allocation patterns, J is a critical factor when multiple schedulers are compared. With the DFT constraints and Assumption 1, it is clear to see that both the total number of RB allocation patterns, J, and the problem search space are significantly reduced.

V. Numerical Results

A. Simulation Setup

In this section, we present the simulation results for the α-fair, SRM, PF, and MMF schedulers in a multi-cell multiuser scenario. Our goal is to identify the efficiency and fairness trade-offs of these schedulers along with the characterization of the aggregate user rate and power. In our simulation model, we consider 19 macrocells, in which each cell is employed with 3-sector antennas. The users are randomly dropped within the macrocell sector area and each user is equipped with a single omni-directional antenna. We investigate a range of user numbers from 2 to 16. Furthermore, we consider that all users are always active and have data to transmit. This model is known as the full buffer traffic model [15]. Also, shadow fading of a user to each base station is considered to be spatially correlated, and the procedure to generate this parameter is detailed in [14]. Shadow fading parameters among different users are assumed to be uncorrelated, although in practice if mobiles are close to each other, this would not hold [14]. The simulation models and parameters are summarized in Table I. These are in accordance with the standard models and baseline simulation setups in [14], [15]. We assume an uplink system with a bandwidth of 10 MHz, and included frequency selective fading in order to observe the effects of channel dependent scheduling. It is assumed that the power delay profile follows the modified Pedestrian B channel model in [14]. The channel state is assumed to be static during a frame and it is independent from one to another. We consider $b_1 = 0.75$ and $b_2 = 1.25$ as suggested in [25]. Finally, the wrap-around technique is used to avoid edge effects.

In each simulation, the data are collected from all 57 cells and the experiment is repeated 10 times to obtain reliable statistics. As discussed in Section II, noncooperative schedulers are used at each base station. In particular, we investigate five properties of each scheduler: the price of fairness, the fairness index, the aggregate user rates, the cumulative distribution function (c.d.f) of user rates, and the aggregate power. We use the fairness index definition in [21] such that $F = (\sum_{k=1}^{K_c} C_k(\gamma))^2/(K_c \sum_{k=1}^{K_c} C_k^2(\gamma))$. It attains its maximum value 1 when each user has the same data rate, and its minimum value $1/K_c$ when all the resources are allocated to a single user only.

TABLE I
Simulation Parameters

Parameter	Setting
Cell layout	Hexagonal grid, 19 cells, 3-sectors per site
Channel bandwidth	10 MHz
Carrier frequency	2 GHz
Freq. selective channel model	Pedestrian B Model
Path loss model	$128.1 + 37.6 \log_{10}(d)$
Inter-site distance	500 m
Total number of RBs	50 RBs
Maximum UE power	23 dBm
Uplink power control: P_0 and β	-60 dBm and 0.8
Effective thermal noise power	-174 dBm/Hz
Base station noise figure	5 dB
Base station antenna gain	15 dBi
UE transmit antenna gain	0 dBi
Antenna horizontal pattern, $A(\theta)$	$-\min(12(\theta/\theta_{3\text{dB}})^2, A_m)$
A_m, $\theta_{3\text{dB}}$	20 dB, 70°
Penetration loss	20 dB
Macrocell MCL	70 dB
Shadow fading std. dev.	8 dB
Site-to-site fading correlation	0.5
Traffic model	Full buffer

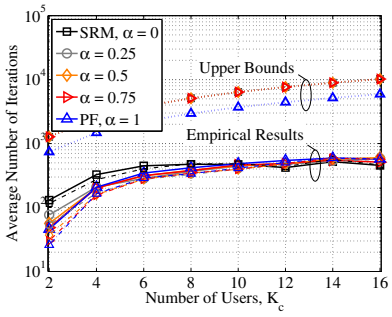

Fig. 4. The average number of iterations to solve the root problems are depicted for the theoretical upper bounds (dotted), and the empirical results considering the DFT constraints (dashed-lines) and without these constraints (solid lines).

B. Optimization Setup

To solve the optimization problems, we used IBM ILOG CPLEX Optimization Studio v12.4. This tool employs the dynamic search method, a variant of the branch-and-cut method [35]. In the branch-and-cut method, the binary integer problem is first reduced to the LP problem by relaxing the binary integer constraint. The relaxed LP problem is referred to as the root problem, and used as a starting point to divide the main problem into subproblems. The solution to the root problem provides the upper bound for the solution to the binary integer problem. By introducing new cuts, using methods such as cutting-plane algorithms, new subproblems are formed until the integer solution that maximizes the objective is obtained.

The average number of iterations required to solve the root problem is no more than $(JK_c/2)$ for the binary integer problems [34, p. 128]. Unfortunately, we cannot provide any upper bounds for the mixed integer problem used to solve the

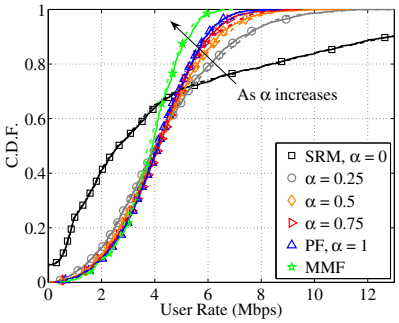

Fig. 5. The c.d.f. of user rates for different schedulers are depicted.

MMF scheduler. Fig. 4 depicts the empirical results for the average number of iterations to solve the root problems for the α-fair, SRM, and PF schedulers. The bounds on the average number of iterations are also shown in Fig. 4. In general, we observe that as the number of users increases, the problem size and the average number of iterations to find the solution for the root problem increase. Also, we note that when the DFT constraints are considered, we do not observe a significant reduction in the average number of iterations to solve the root problems compared to the case without these constraints.

C. Numerical Evaluation

Fig. 5 summarizes the c.d.f. of user rates for different schedulers for $K_c = 8$ users. First, we observe that the c.d.f. of each scheduler with DFT constraints (dashed-lines) closely follows the performance of each scheduler without any constraints (solid lines). Second, we can clearly see the user rate starvation case for the SRM scheduler. On average, 9% of the users do not get any resources with the SRM scheduler. On the other hand, cell-center users achieve significantly more rates with the SRM scheduler, especially in the region above the 70th percentile. Second, we observe that the PF scheduler improves user rates at and below the median, and those rates typically correspond to the cell-edge and median users. For instance, when we look at 5, 10, and 50th percentile user rates, the PF schedulers provide 1.63, 2.17, and 4.13 Mbps, respectively. The SRM scheduler only achieves 0.53 and 2.64 Mbps for 10 and 50th percentile users. Around 70th percentile, the cross-over occurs, and the SRM scheduler starts to provide higher rates compared to the PF scheduler. Third, the MMF scheduler assigns most of the resources to the cell-edge users to maximize the rate for the minimum rate user, and this significantly reduces the median and cell-center user rates. Note that these results are expected since the fairness in the cellular radio networks corresponds to the trade-off between the rates provided to cell-edge and cell-center users. Thus, on the two edges of the efficiency and fairness trade-off lies the SRM and MMF schedulers, respectively, and the PF scheduler balances both properties.

In Fig. 6(a)-(b), the aggregate user rates and the price of fairness for each scheduler are depicted for various number of users per sector. First, we observe that the performance losses incurred by considering the DFT constraints are almost negligible for each scheduler in both figures. In Fig. 6(a), we depict the aggregate user rates of each scheduler for different number of users. This plot also demonstrates the multiuser diversity such that as the number of users increases, the aggregate user rate increases. In Fig. 6(b), we observe that the price of fairness of the α-fair schedulers (for $\alpha \leq 1$) are less than 0.2 in a multi-cell multiuser scenario. Unfortunately, the upper bounds for the price of fairness of most α-fair schedulers ($\alpha > 0.25$) are loose. This is due to the large B/L factor discussed in Section III-B. However, we observe that the bounds are tighter for the $\alpha = 0.25$ case. The price of fairness values for the MMF scheduler are significantly high such that it ranges between 0.1-0.3. Notice that this means that the system efficiency loss between the SRM and MMF scheduler is between 10-30%. Also, it needs to be emphasized that Figs. 6(a)-(b) are closely related with each other. The percentage loss in the aggregate user rates depicted in Fig. 6(a) is, in fact, the price of fairness of each scheduler in Fig. 6(b) compared to the aggregate user rate of the SRM scheduler. Thereby, we can argue that the price of fairness metric gives the network operator a meaningful and reliable metric to compare the efficiencies of any schedulers.

Fig. 6(c) depicts the fairness of each scheduler versus the number of users. Previously in Section III, we discussed that as α increases, the fairness increases as well. We can observe this in Fig. 6(c). The α-fair and MMF schedulers provide highly fair distribution of user rates compared to the SRM scheduler. The fairness of the α-fair schedulers ($\alpha > 0$) ranges between 0.7 and 0.9, whereas the fairness of the SRM scheduler is always less than 0.6. Moreover, the fairness gradually decreases as the number of users increase for the SRM scheduler. This is due to the fact that as the number of users increase, it is more probable that the SRM scheduler allocates more RBs to the users with good channel conditions, and only a few RBs are scheduled to cell-edge users in order to increase the aggregate data rate. At the worst case, the fairness of the SRM schedulers is 0.34 for $K_c = 16$ users, and at this point, the PF scheduler provides roughly three times more fair distribution of user rates compared to the SRM scheduler.

Fig. 6(d) shows the aggregate uplink transmit power versus the number of users for each scheduler. Note that the total dissipated power at UEs is a critical factor due to battery life concerns. We observe that the SRM scheduler always results in an allocation where significantly less power is required compared to the other schedulers. This is due to the fact that the SRM scheduler does not necessarily allocate resources to the cell-edge users that have high path loss values. Therefore, it avoids cases where cell-edge users transmit at high power levels. Also, the gap between the aggregate power of SRM and other schedulers gradually increases as the number of users increase.

VI. Conclusion

In this paper, we investigated the uplink resource scheduling problem for SC-FDMA systems. We studied a family of utility functions called as the α-fair utility function. In particular, we focused on the SRM, PF, and MMF schedulers, and highlighted the system efficiency, fairness, and power trade-offs. We identified that the DFT implementation constraints result in only a slight degradation in the system efficiency and fairness. We introduced a general framework to compare the

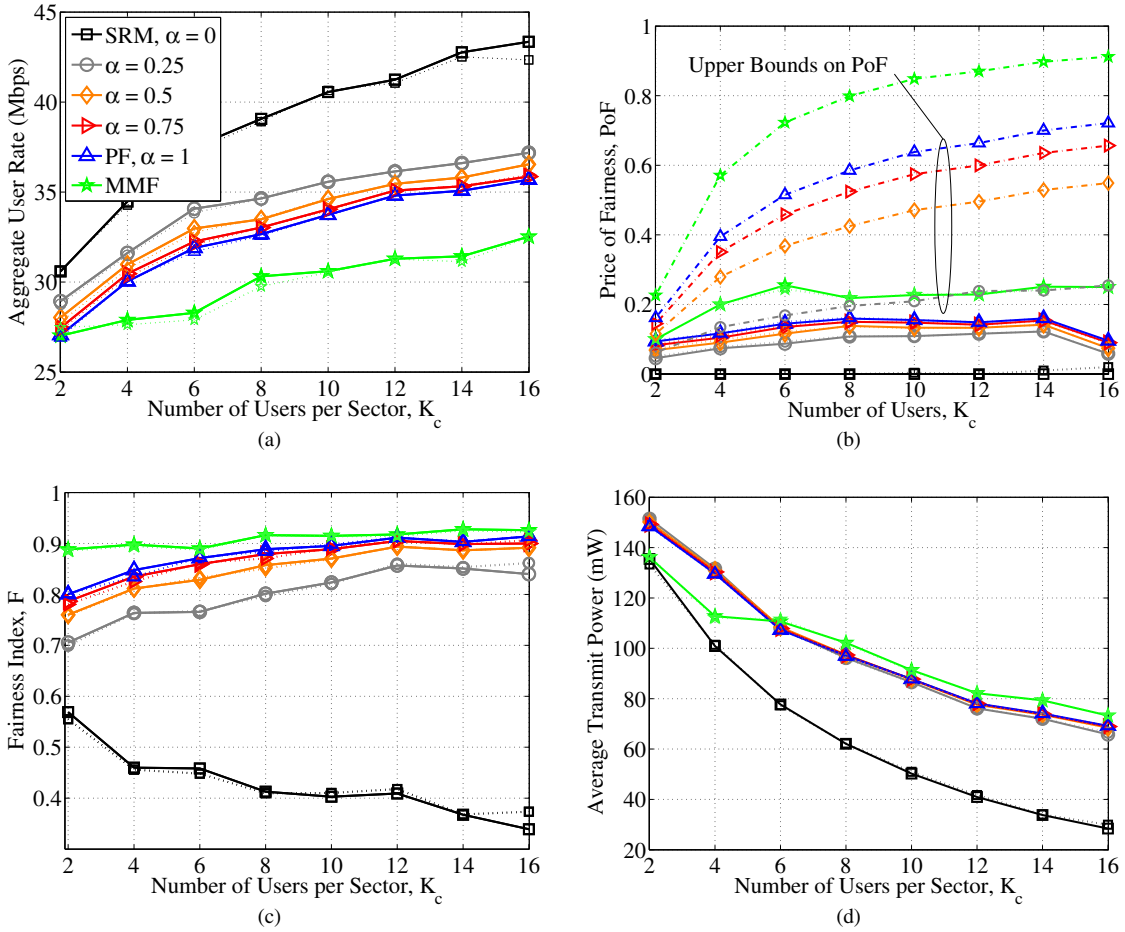

Fig. 6. The aggregate user rates, price of fairness, fairness index, and aggregate user transmit power are depicted in (a)-(d), respectively, for different schedulers in a multi-cell multiuser scenario. Solid lines indicate the performance of each scheduler without any constraints, and the dashed-lines are for the schedulers with DFT constraints.

performance of different schedulers by using concise metrics such as the price of fairness and fairness index. We observed that the α-fair schedulers for $\alpha > 0$ provide fairer distributions of resources at the cost of some efficiency losses and increased transmit power. However, finding the appropriate α parameter that satisfies the QoS constraints and improves the cell-edge user rates is a challenge. The analysis presented in this paper provides network operators with a greater provisioning to identify these trade-offs associated with resource allocation for different schedulers and optimize the user experience in the system. Although it is not considered in this work, the frequency domain schedulers investigated here can be used to complement time domain schedulers. This would require an appropriate weighting rule, including the past user rates over a time window, in the scheduling objective. Thereby, different QoS requirements of each user such as delay and guaranteed bit rate, possibly due to different types of applications, can be included in the scheduling algorithm.

REFERENCES

[1] Cisco Systems, Inc., "Cisco Visual Networking Index: Global mobile data traffic forecast update, 2012-2017," White Paper, Feb. 2013.

[2] H. Holma and A. Toskala, *LTE for UMTS, OFDMA and SC-FDMA Based Radio Access*. Wiley, 2009.

[3] D. Bertsimas, V. F. Farias, and N. Trichakis, "The price of fairness," *Operations Research*, vol. 59, no. 1, pp. 17–31, Jan.-Feb. 2011.

[4] ——, "On the efficiency-fairness trade-off," *Management Science*, vol. 58, no. 12, pp. 2234–2250, Dec. 2012.

[5] P. Duhamel and M. Vetterli, "Fast Fourier transforms: a tutorial review and a state of the art," *Signal Process.*, vol. 19, no. 4, pp. 259–299, Apr. 1990.

[6] Ericsson, "DFT size for uplink transmissions," 3GPP, TSG RAN WG1 Meeting 46, Seoul, Korea, R1-062852, Oct. 2006.

[7] S. B. Lee, I. Pefkianakis, A. Meyerson, S. Xu, and S. Lu, "Proportional fair frequency-domain packet scheduling for 3GPP LTE uplink," in *Proc. 2009 IEEE INFOCOM*, pp. 2611–2615.

[8] I. C. Wong, O. Oteri, and W. McCoy, "Optimal resource allocation in uplink SC-FDMA systems," *IEEE Trans. Wireless Commun.*, vol. 8, no. 5, pp. 2161–2165, May 2009.

[9] J. Lim, H. G. Myung, K. Oh, and D. J. Goodman, "Proportional fair scheduling of uplink single-carrier FDMA systems," in *Proc. 2006 IEEE Personal, Indoor Mobile Radio Commun.*

[10] ——, "Channel-dependent scheduling of uplink single carrier FDMA systems," in *Proc. 2006 IEEE Veh. Technol. Conf.*

[11] L. R. Temino, B. Gilberto, S. Frattasi, and P. Mogensen, "Channel-aware scheduling algorithms for SC-FDMA in LTE uplink," in *Proc. 2008 IEEE Personal, Indoor Mobile Radio Commun.*

[12] K. Elgazzar, M. Salah, A.-E. M. Taha, and H. Hassanein, "Comparing uplink schedulers for LTE," in *Proc. 2010 Int. Wireless Commun. Mobile Comput. Conf.*, pp. 189–193.

[13] H. Safa and K. Tohme, "LTE uplink scheduling algorithms: performance and challenges," in *Proc. 2012 Int. Conf. Telecommun.*, pp. 1–6.

[14] 3GPP, TR 25.996, "Spatial channel model for multiple input multiple output (MIMO) simulations (Release 11)," Tech. Rep., Sept. 2012.

[15] 3GPP, TR 36.814, "Further advancements for E-UTRA physical layer aspects (Release 9)," Tech. Rep., Mar. 2010.

[16] S. Schwarz, C. Mehlführer, and M. Rupp, "Low complexity approximate

maximum throughput scheduling for LTE," in *Proc. 2010 Asilomar Conf.*, pp. 1563–1569.
[17] G. Song and Y. Li, "Cross-layer optimization for OFDM wireless networks—part I: theoretical framework," *IEEE Trans. Wireless Commun.*, vol. 4, no. 2, pp. 614–624, Mar. 2005.
[18] ——, "Cross-layer optimization for OFDM wireless networks—part II: algorithm development," *IEEE Trans. Wireless Commun.*, vol. 4, no. 2, pp. 625–634, Mar. 2005.
[19] P. Ameigeiras, Y. Wang, J. Navarro-Ortiz, P. Mogensen, and J. Lopez-Soler, "Traffic models impact on OFDMA scheduling design," *EURASIP J. Wireless Commun. Netw.*, no. 1, pp. 1–13, Feb. 2012.
[20] K. Davaslioglu and E. Ayanoglu, "Interference-based cell selection in heterogenous networks," in *Proc. 2013 IEEE Inf. Theory Applications Workshop*, pp. 1–6.
[21] R. Jain, *The Art of Computer Systems Performance Analysis: Techniques for Experimental Design, Measurement, Simulation, and Modeling*. Wiley, 1991.
[22] 3GPP, TS 36.213, "Physical layer procedures (Release 10)," Tech. Rep., July 2012.
[23] H. G. Myung and D. J. Goodman, *Single Carrier FDMA: A New Air Interface for Long Term Evolution*. Wiley, 2008.
[24] Motorola, "Simulation methodology for E-UTRA UL, IFDMA and DFT-Spread OFDMA," 3GPP, RAN1 Meeting 43, Seoul, Korea, R1-051335, Nov. 2005.
[25] P. Mogensen, W. Na, I. Kovacs, F. Frederiksen, A. Pokhariyal, K. Pedersen, T. Kolding, K. Hugl, and M. Kuusela, "LTE capacity compared to the Shannon bound," in *Proc. 2007 IEEE Veh. Technol. Conf.*, pp. 1234–1238.
[26] Z. Han, D. Niyato, W. Saad, T. Başar, and A. Hjørungnes, *Game Theory in Wireless and Communication Networks: Theory, Models, and Applications*. Cambridge University Press, 2012.
[27] J. Mo and J. Walrand, "Fair end-to-end window-based congestion control," *IEEE/ACM Trans. Netw.*, vol. 8, no. 5, pp. 556–567, Oct. 2000.
[28] F. Kelly, "Charging and rate control for elastic traffic," *Eur. Trans. Telecommun.*, vol. 8, pp. 33–37, Jan./Feb. 1997.
[29] P. Viswanath, D. Tse, and R. Laroia, "Opportunistic beamforming using dumb antennas," *IEEE Trans. Inf. Theory*, vol. 48, no. 6, pp. 1277–1294, June 2002.
[30] A. Tang, J. Wang, and S. Low, "Counter-intuitive throughput behaviors in networks under end-to-end control," *IEEE/ACM Trans. Netw.*, vol. 14, no. 2, pp. 355–368, Apr. 2006.
[31] NEC Group, "DFT size," 3GPP, TSG RAN WG1 Meeting 47, Riga, Latvia, R1-063199, Nov. 2006.
[32] 3GPP, TS 36.211, "Physical channels and modulation (Release 11)," Tech. Rep., Sept. 2012.
[33] D. P. Bertsekas, *Nonlinear Programming*. Athena Scientific, 1995.
[34] D. Bertsimas and J. N. Tsitsiklis, *Introduction to Linear Optimization*. Athena Scientific, 1997.
[35] IBM ILOG, "IBM ILOG CPLEX optimization studio CPLEX user's manual," Version 12, Release 4, 2011.

Kemal Davaslioglu (S '06) received the B.S. degree from Bilkent University, Ankara, Turkey, in 2008 and the M.S. degree from Bogazici University, Istanbul, Turkey, in 2010, both in electrical engineering. He is currently pursuing his Ph.D. degree in the Department of Electrical Engineering and Computer Science, University of California, Irvine, CA where he is affiliated with the Center for Pervasive Communications and Computing. From 2011 to 2012, he was with Broadcom Corp., Irvine, CA, working on 10-Gigabit Ethernet systems. His research interests include resource allocation, load balancing, and energy-efficiency in next-generation mobile wireless networks, wireless communication theory, signal processing for wireless communications, and ultra-wideband communications.

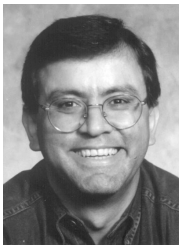

Ender Ayanoglu (S82-M85-SM90-F98) received the B.S. degree from the Middle East Technical University, Ankara, Turkey, in 1980, and the M.S. and Ph.D. degrees from Stanford University, Stanford, CA, in 1982 and 1986, respectively, all in electrical engineering. He was with the Communications Systems Research Laboratory, part of AT&T Bell Laboratories, Holmdel, NJ until 1996, and Bell Labs, Lucent Technologies until 1999. From 1999 until 2002, he was a Systems Architect at Cisco Systems, Inc. Since 2002, he has been a Professor in the Department of Electrical Engineering and Computer Science, University of California, Irvine, where he served as the Director of the Center for Pervasive Communications and Computing and held the Conexant-Broadcom Endowed Chair during 2002- 2010. Dr. Ayanoglu is the recipient of the IEEE Communications Society Stephen O. Rice Prize Paper Award in 1995 and the IEEE Communications Society Best Tutorial Paper Award in 1997. From 1993 until 2014, he was an Editor of the IEEE TRANSACTIONS ON COMMUNICATIONS and served as its Editor-in-Chief from 2004 to 2008. Currently, he is serving as a Senior Editor of the same journal. From 1990 to 2002, he served on the Executive Committee of the IEEE Communications Society Communication Theory Committee, and from 1999 to 2001, was its Chair.